Numerical methods for biomedical problems posed on surfaces and bulk-surface coupled problems

A.Chernyshenko,M.Olshanskii

INM RAS

Moscow, INM RAS, 31.10.2016

PDEs posed on surfaces or systems of coupled bulk–surface PDEs arise in many engineering and natural science applications:

- diffusion along grain boundaries
- multiphase fluid dynamics with soluble or insoluble surfactants
- the transport of solute in fractured porous media
- dynamics of biomembranes
- crystal growth
- signaling in biological networks
- brain warping
- fluids in lungs
- etc.

In these and other applications, advection–diffusion–reaction or fluid equations defined in a volume domain are coupled to another advection–diffusion–reaction equations posed on a surface. The surface may be embedded in the bulk or belong to a boundary of the volume domain.

PDEs posed on surfaces or systems of coupled bulk–surface PDEs arise in many engineering and natural science applications:

- diffusion along grain boundaries
- multiphase fluid dynamics with soluble or insoluble surfactants
- the transport of solute in fractured porous media
- dynamics of biomembranes
- crystal growth
- signaling in biological networks
- brain warping
- fluids in lungs
- etc.

In these and other applications, advection–diffusion–reaction or fluid equations defined in a volume domain are coupled to another advection–diffusion–reaction equations posed on a surface. The surface may be embedded in the bulk or belong to a boundary of the volume domain.

PDEs posed on surfaces or systems of coupled bulk–surface PDEs arise in many engineering and natural science applications:

- diffusion along grain boundaries
- multiphase fluid dynamics with soluble or insoluble surfactants
- the transport of solute in fractured porous media
- dynamics of biomembranes
- crystal growth
- signaling in biological networks
- brain warping
- fluids in lungs
- etc.

In these and other applications, advection–diffusion–reaction or fluid equations defined in a volume domain are coupled to another advection–diffusion–reaction equations posed on a surface. The surface may be embedded in the bulk or belong to a boundary of the volume domain.

- Lipid molecules may aggregate into a bilayer or membrane which forms an encapsulating bag called vesicle. Lipid membranes are ubiquitous in biological systems, and an understanding of vesicles provides an important element to understand real cells.
- Equilibrium shapes discarding the effect of the bulk fluid are obtained by minimizing the surface bending energy under area and volume constraints. There exists a biomembrane model which incorporates the effect of the bulk fluid.

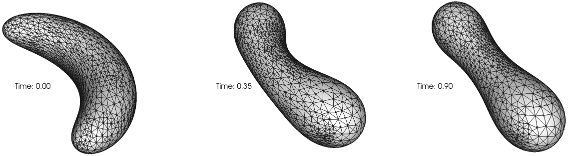

Рис.: Evolution of an initial non axisymmetric 3D banana shaped volume mesh subject to the high inertia flow

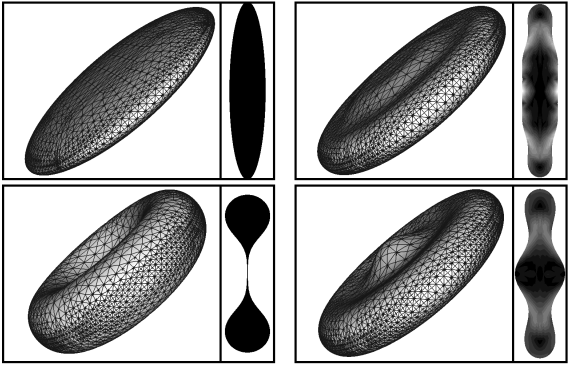

Biomembrane fluid model evolution. Each frame shows the membrane mesh and a symmetry cut along a big axis.

A. Bonito, R. Nochetto, and M. Pauletti. *Dynamics of biomembranes: effect of the bulk fluid*, 2011

Numerical treatment of bulk-surface coupled PDEs

Different approaches can be distinguished depending on how the surface is recovered and equations are treated.

- Fitted FEM: tetrahedral mesh fits the surface + FEM
  - advection-diffusion (Elliott, Ranner, 2013)
  - non-linear reaction-diffusion (Madzvamuse, Chung, 2015,2016)
  - two-phase flow with surfactants (Barrett, Garcke,Nurnberg, 2015)
- Unfitted FEM: surface cuts through the background tetrahedral mesh
  - cutFEM, Nitsche-XFEM, trace FEM (Burman et al, 2015; Olshanskii, Reusken, Xu, 2014)
  - advection-diffusion (Gross, Olshanskii, Reusken, 2014)
  - two-phase Stokes flow with soluble surfactants (Hansbo, Larson, Zahedi, 2015)
  - time-dependent domains (Hansbo, Larson, Zahedi, 2016)
- FV/FD in bulk domain + FEM (triangulation/extend the PDE of the surface to a narrow band)

Numerical treatment of bulk-surface coupled PDEs

Goals:

1. to allow the surface to overlap with the background mesh in an arbitrary way
2. avoid regular triangulating the surface
3. do not use any extension of the surface PDE to the bulk domain

Approaches:

- octree meshes with cut-cells
- MPFA - nonlinear FV method for polyhedral meshes (Lipnikov, Svyatskiy, Vassilevski, 2012; Chernyshenko, Vassilevski, 2014)
- trace FEM on octree meshes (Chernyshenko, Olshanskii, 2015)

Also receive:

- surface parametrization is not required
- only degrees of freedom from the cells cut by the surface are active

Assume the given bulk domain $\Omega \in \mathbb{R}^3$ and a piecewise smooth surface $\Gamma \subset \Omega$, assume $\partial\Gamma \subset \partial\Omega$. u_i - volume concentration Ω_i, v - surface concentration along Γ .
Equations in subdomains:

$$
\begin{aligned}
\phi_i \frac{\partial u_i}{\partial t} + \mathrm{div}(\mathbf{w}_i u_i) - D_i \Delta u_i &= f_i \quad \text{in } \Omega_i, \\
u_i &= v \quad \text{on } \partial\Omega_i \cap \Gamma
\end{aligned} \tag{1}
$$

On the surface Γ:

$$
\phi_\Gamma \frac{\partial v}{\partial t} + \mathrm{div}_\Gamma(\mathbf{w}_\Gamma v) - dD_\Gamma \Delta_\Gamma v = F_\Gamma(u) + f_\Gamma \quad \text{on } \Gamma, \tag{2}
$$

where $\nabla_\Gamma g = \nabla g - \nabla g \cdot \mathbf{n}_\Gamma \mathbf{n}_\Gamma$, $f_\Gamma \in L^2(\Gamma)$, $\mathbf{w}_\Gamma \in H^{1,\infty}(\Gamma)$, $\phi_i > 0$,$\phi_\Gamma > 0$ - porosity, d - fracture width

The total surface flux $F_\Gamma(u)$ represents the contribution of the bulk to the solute transport in the fracture. The mass balance at Γ leads to the equation

$$F_\Gamma(u) = [-D\mathbf{n}_\Gamma \cdot \nabla u + (\mathbf{n}_\Gamma \cdot \mathbf{w})u]_\Gamma, \tag{3}$$

If Γ is piecewise smooth, then we need further conditions on the edges $\mathcal{E}$.

$$\sum_{i=1}^{M} \mathbf{w}_i = 0 \quad , \sum_{i=1}^{M} d_i D_{\Gamma,i} \frac{\partial v_i}{\partial \mathbf{n}_{\partial\Gamma,i}} = 0 \quad \text{on} \quad \mathcal{E}. \tag{4}$$

Initial and boundary conditions:

$$\begin{cases} \dfrac{\partial u}{\partial \mathbf{n}_{\partial\Omega}} = 0 \quad \text{on } \partial\Omega_N, \\ \qquad u = u_D \quad \text{on } \partial\Omega_D, \\ u\big|_{t=0} = u_0 \quad \text{in } \Omega, \end{cases} \qquad \begin{cases} \dfrac{\partial v}{\partial \mathbf{n}_{\partial\Gamma}} = 0 \quad \text{on } \partial\Gamma_N, \\ \qquad v = v_D \quad \text{on } \partial\Gamma_D, \\ v\big|_{t=0} = v_0 \quad \text{on} \quad \Gamma. \end{cases} \tag{5}$$

Octree meshes with cut-cells (Chernyshenko A., 2013) - modification of Multimaterial marching cubes (Wu Z., Sullivan J.M., 2003) and Cubical marching squares (C.-C. Ho, F.-C.Wu, et al, 2005) algorithms

- $\mathcal{T}_h$ - volume octree mesh in Ω
- Γ intersects $\mathcal{T}_h$ in arbitrary way.
- Γ_h - irregular triangulation of Γ (*2nd order) is used for integration only. Divides Ω into $\Omega_{i,h}$.

Finally we get a polyhedral mesh (hexahedra + polyhedra)

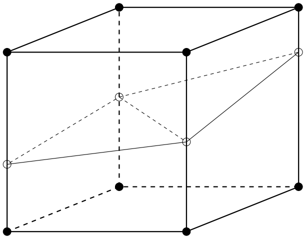

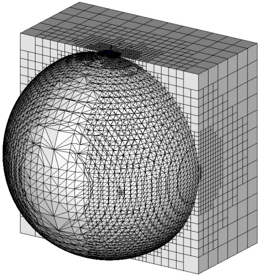

Monotone FV method for the advection-diffusion equations

- 3D advection: Nikitin K., Vassilevski Yu. , 2010
- 3D diffusion: Chernyshenko A., Vassilevski Yu. , 2013

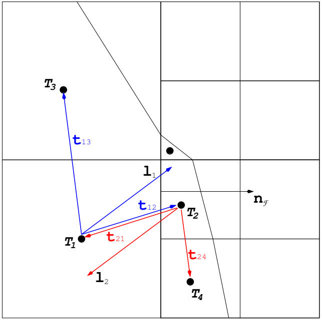

- nonlinear
- compact stencil
- monotone (DMP)
- *2nd order in concentrations

Approaches. 2D: The trace finite element method.

- V_h - volumetric finite element space .
  $V_h := \{v_h \in C(\Omega) \mid v_h|_S \in Q_1 \;\; \forall\, S \in \mathcal{T}_h\}$, where Q_1 -all piecewise trilinear continuous functions with respect to the bulk octree mesh $\mathcal{T}_h$.
- V_h^Γ - the space of traces on Γ_h of all piecewise trilinear continuous functions with respect to the outer triangulation $\mathcal{T}_h$
  $V_h^\Gamma := \{\psi_h \in H^1(\Gamma_h) \mid \exists\; v_h \in V_h$ such that $\psi_h = v_h|_{\Gamma_h}\}$.
- FE-discretization of (2): Find $v_h \in V_h^\Gamma$ such that

$$\int_{\Gamma_h} \left(\phi_{\Gamma,h} \frac{\partial v_h}{\partial t} w_h + d_h D_{\Gamma,h} \nabla_{\Gamma_h} v_h \cdot \nabla_{\Gamma_h} w_h + (\mathbf{w}_h \cdot \nabla_{\Gamma_h} v_h) w_h \right) + (\mathrm{div}_{\Gamma_h} \mathbf{w}_h)\, u_h v_h \mathrm{d}\mathbf{s}_h = \int_{\Gamma_h} (F_{\Gamma,h}(u_h) + f_{\Gamma,h}) w_h \,\mathrm{d}\mathbf{s}_h \quad (6)$$

for all $w_h \in V_h^\Gamma$

A.Y.Chernyshenko, M.A. Olshanski, *An adaptive octree finite element method for PDEs posed on surfaces*, 2015.

Numerical examples. Surface PDE on compicated geometry

$$\phi(\mathbf{x}) = \frac{1}{4}x_1^2 + x_2^2 + \frac{4x_3^2}{(1+\frac{1}{2}\sin(\pi x_1))^2} - 1.$$

$\mathbf{w} = 0$, $\varepsilon = 1$, $c = 1$, $u = x_1 x_2$ on Γ.

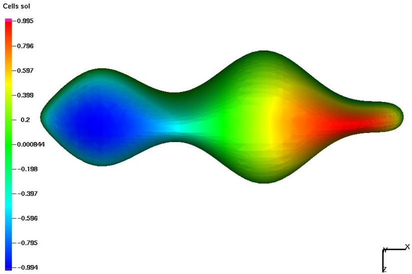

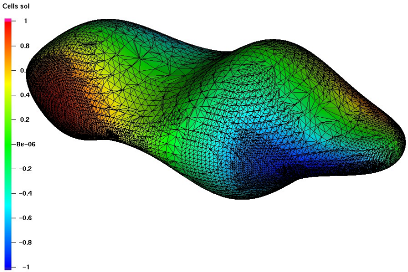

G. Dziuk and C. M. Elliott, *Finite element methods for surface PDEs*, Acta Numerica (2013).

Numerical examples. Surface PDE on compicated geometry

$$\phi(\mathbf{x}) = \frac{1}{4}x_1^2 + x_2^2 + \frac{4x_3^2}{(1+\frac{1}{2}\sin(\pi x_1))^2} - 1.$$

$\mathbf{w} = 0$, $\varepsilon = 1$, $c = 1$, $u = x_1 x_2$ on Γ.

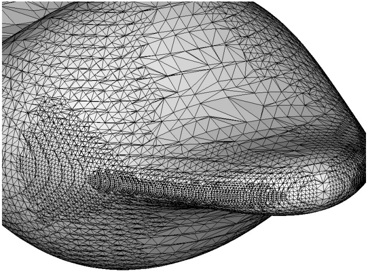

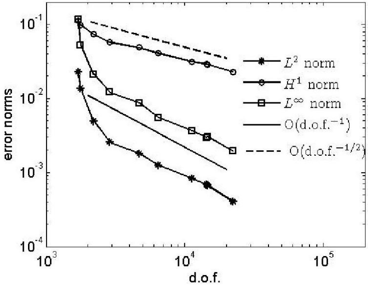

Γ - unit sphere envolved in the cube $\Omega = [-1,1]^3$
The velocity field on Γ

$$\mathbf{w}(\mathbf{x}) = (-x_2\sqrt{1-x_3^2}, x_1\sqrt{1-x_3^2}, 0)^T,$$

The velocity field in Ω_i : $\mathbf{w}_i(\mathbf{x}) = \mathbf{w}(\mathbf{x}) + \theta\mathbf{s}_i$, where $\theta = 0.1$, $\mathbf{s}_1 = (1,1,0)$, $\mathbf{s}_1 = (2,1,0)$.
The exact solution on the sphere: $v(\mathbf{x}) = x_1 x_2 \arctan\left(\frac{2x_3}{\sqrt{\varepsilon}}\right)$.
The exact solution in subdomains:

$$u_1(\mathbf{x}) = v(\mathbf{x}) \cdot \exp(1 - x^2 - y^2 - z^2), \qquad u_2(\mathbf{x}) = v(\mathbf{x}).$$

We consider the case when $\varepsilon = 1$.

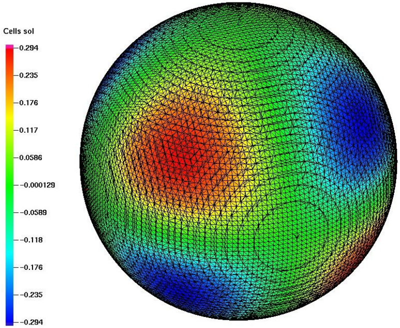
Cells sol
0.294
0.235
0.176
0.117
0.0586
-0.000129
-0.0589
-0.118
-0.176
-0.235
-0.294

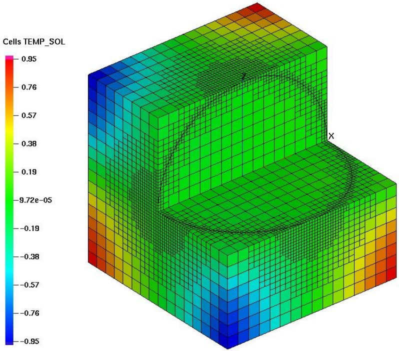
Cells TEMP_SOL
0.95
0.76
0.57
0.38
0.19
9.72e-05
-0.19
-0.38
-0.57
-0.76
-0.95
X

	#d.o.f.	L^2-norm	H^1-norm	L^∞-norm
3D	120	1.139e-2	1.447e-1	2.817e-2
	3576	3.457e-3	5.602e-2	2.582e-2
	74176	9.631e-4	2.111e-2	7.609e-3
2D	100	1.043e-2	1.020e-1	1.938e-2
	1628	1.506e-3	5.118e-2	6.467e-3
	26724	6.134e-4	2.652e-2	3.980e-3

$\Omega = [0,1]^3$, $\Gamma = \Gamma_{12} \cup \Gamma_{13} \cup \Gamma_{23}$ - divides Ω into three parts
Consider functions

$$\phi_1 = \begin{cases} 16(y-y_0)^4, & y > y_0 \\ 0, & y \le y_0 \end{cases}$$

and $\phi_2 = x - y$, $\phi_3 = x + y - 1$.
For the exact solution which is continuous but has derivative jump we take the function

$$\begin{cases} u_1 = & \sin(2\pi z) \cdot \phi_2 \cdot \phi_3 & \text{in } \Omega_1 \\ u_2 = & \sin(2\pi z) \cdot \phi_1 & \text{in } \Omega_2 \\ u_3 = & \sin(2\pi z) 2x \cdot \phi_1 & \text{in } \Omega_3 \end{cases}$$

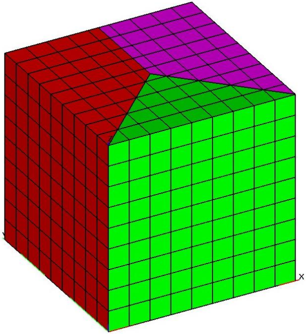

$\Omega = [0,1]^3$, $\Gamma = \Gamma_{12} \cup \Gamma_{13} \cup \Gamma_{23}$ - divides Ω into three parts
Consider functions

$$\phi_1 = \begin{cases} 16(y-y_0)^4, & y > y_0 \\ 0, & y \le y_0 \end{cases}$$

and $\phi_2 = x - y$, $\phi_3 = x + y - 1$.
For the exact solution which is continuous but has derivative jump we take the function

$$\begin{cases} u_1 = & \sin(2\pi z) \cdot \phi_2 \cdot \phi_3 & \text{in } \Omega_1 \\ u_2 = & \sin(2\pi z) \cdot \phi_1 & \text{in } \Omega_2 \\ u_3 = & \sin(2\pi z) 2x \cdot \phi_1 & \text{in } \Omega_3 \end{cases}$$

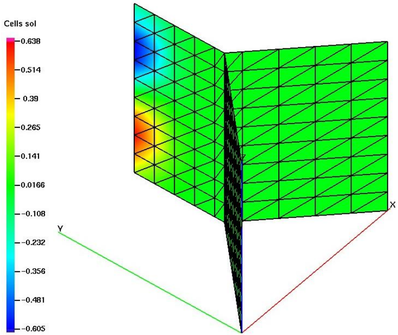

Таблица: Convergence of numerical solutions

	#d.o.f.	L^2-norm	rate	L^∞-norm	rate
3D	855	6.374e-3		3.920e-2	
	7410	1.698e-3	1.84	1.276e-2	1.56
	61620	4.235e-4	1.97	3.506e-3	1.83
	502440	1.044e-4	2.00	1.129e-3	1.62
2D	232	8.469e-3		9.280e-3	
	1242	2.003e-3	1.72	2.779e-3	1.44
	5662	5.588e-4	1.69	1.217e-3	1.09
	24102	1.791e-4	1.58	5.181e-4	1.18

Next we rotate the fracture around the line $x = 0.5, z = 0.5$ by angle α.

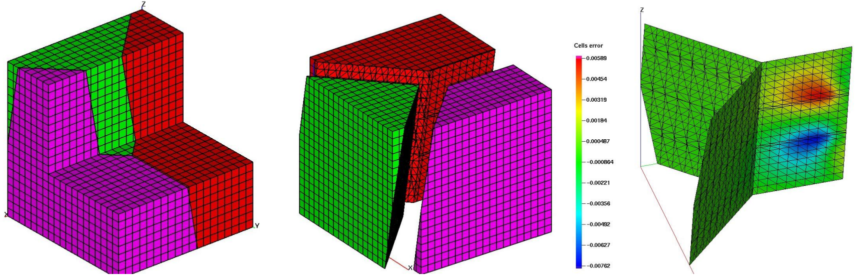

Рис.: $\alpha = 20$. 3D mesh, error on rotated fracture (right)

Next we rotate the fracture around the line $x = 0.5, z = 0.5$ by angle α.

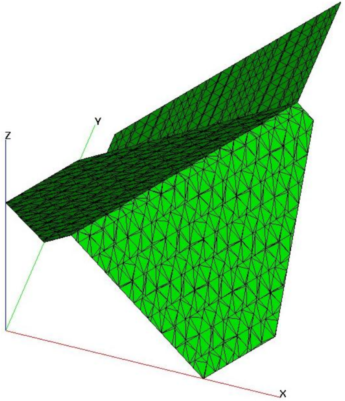

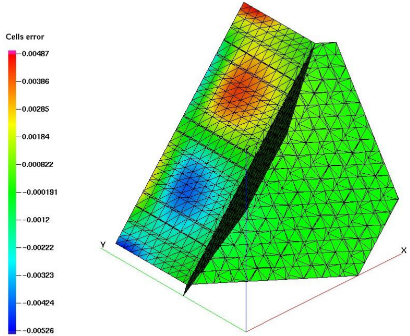

Рис.: $\alpha = 40$. 2D mesh, error on rotated fracture (right

Next we rotate the fracture around the line $x = 0.5, z = 0.5$ by angle α.

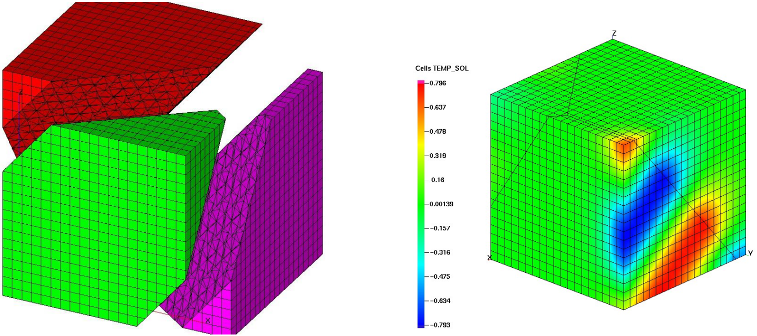

Рис.: $\alpha = 40$. 3D mesh, solution on 3D mesh

Таблица: Convergence of numerical solutions. $\alpha = 20$

	#d.o.f.	L^2-norm	rate	L^∞-norm	rate
3D	965	6.319e-3		3.754e-2	
	7872	1.805e-3	1.79	1.280e-2	1.55
	63592	5.623e-4	1.80	3.411e-3	1.90
2D	321	7.792e-3		2.716e-2	
	1692	2.084e-3	1.59	5.400e-3	1.94
	7944	7.019e-4	1.41	2.001e-3	1.29

Таблица: Convergence of numerical solutions. $\alpha = 40$

	#d.o.f.	L^2-norm	rate	L^∞-norm	rate
3D	991	5.934e-3		3.783e-2	
	7996	1.700e-3	1.80	1.276e-2	1.56
	64046	4.907e-4	1.80	3.515e-3	1.86
2D	353	8.167e-3		2.696e-2	
	1932	2.146e-3	1.57	5.566e-3	1.85
	8766	7.115e-4	1.46	2.063e-3	1.31

Boundary conditions: $u_D = 1$ inflow $(y = 1)$, others: $\dfrac{\partial u}{\partial \mathbf{n}_{\partial\Omega}} = 0$ The velocity field: $\mathbf{w} = c(0, -2, 0)$ в Ω и

$$\begin{cases} \mathbf{w}_{\Gamma,1} &= c(0, -5, 0), \\ \mathbf{w}_{\Gamma,2} &= c(-1/\sqrt{2}, -1/\sqrt{2}, 0), \\ \mathbf{w}_{\Gamma,3} &= c(1/\sqrt{2}, -1/\sqrt{2}, 0), \end{cases}$$

For the case of diffusion domination $c = 1/8$, advection-dominated problem $c = 8$.

Numerical examples. Triple fraction, unsteady problem

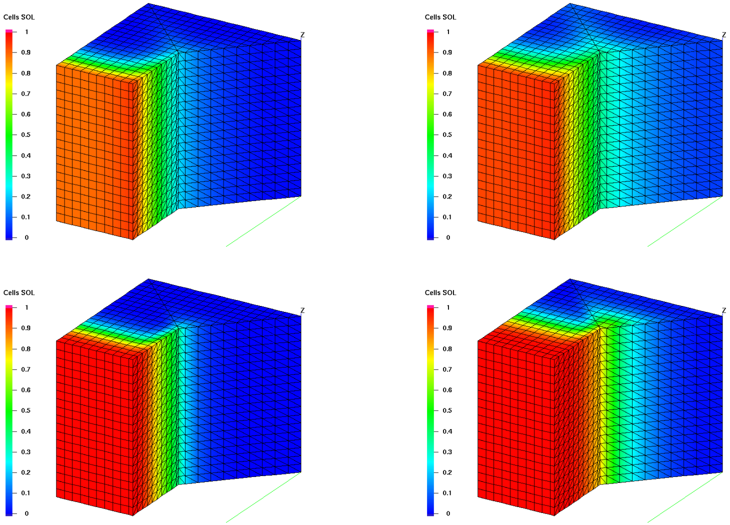

Numerical examples. Triple fraction, unsteady problem

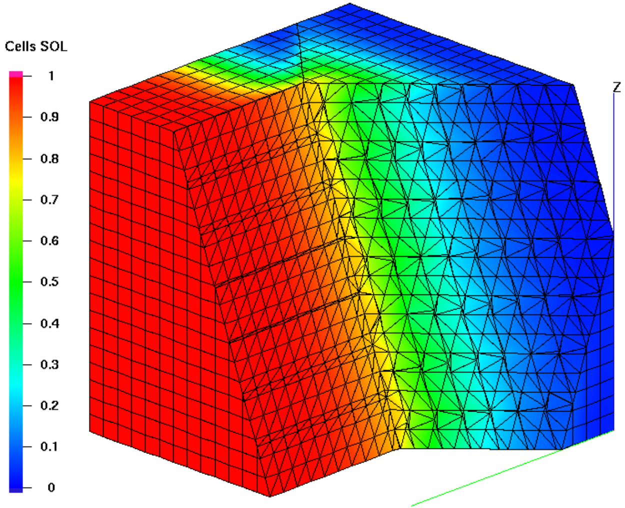

Conclusions

- We studied a trace finite element method for PDEs posed on hypersurfaces and a hybrid FV-FE method for bulk-surface coupled problems
- The mesh is unfitted to a surface
- The method works for surfaces defined implicitly, parametrization of a surface is not required
- The number of active d.o.f. is optimal and comparable to methods in which Γ is meshed directly
- Optimal order of convergence in H^1 and L_2 norms is proved for quasi-uniform bulk grids
- Numerical experiments shows optimal order of convergence

Thank You for attention!